# βD305A Mutant of Tryptophan Synthase Shows Strongly Perturbed Allosteric Regulation and Substrate Specificity†

Davide Ferrari,‡,§ Li-Hong Yang,||,⊥ Edith W. Miles,|| and Michael F. Dunn*,§

*Department of Biochemistry, University of California at Riverside, Riverside, California 92521, and The National Institutes of Health, Laboratory of Biochemistry and Genetics, NIDDK, NIH, Building 8/Room 2A09, Bethesda, Maryland 20892-0830*

*Received December 20, 2000; Revised Manuscript Received April 27, 2001*

ABSTRACT: Substrate channeling in the tryptophan synthase bienzyme is regulated by allosteric interactions. Allosteric signals are transmitted via a scaffolding of structural elements that includes a monovalent cation-binding site and salt-bridging interactions between the side chains of βAsp 305, βArg 141, βLys 167, and αAsp 56 that appear to modulate the interconversion between open and closed conformations. βAsp 305 also interacts with the hydroxyl group of the substrate L-Ser in some structures. One possible functional role for βAsp 305 is to ensure the allosteric transmission that triggers the switching of αβ-dimeric units between open and closed conformations of low and high activity. This work shows that substitution of βAsp 305 with Ala (βD305A) decreases the affinity of the β-site for the substrate L-Ser, destabilizes the enzyme-bound α-aminoacrylate, E(A−A), and quinonoid species, E(Q), and changes the nucleophile specificity of the β-reaction. The altered specificity provides a biosynthetic route for new L-amino acids derived from substrate analogues. βD305A also shows an increased rate of formation of pyruvate upon reaction with L-Ser relative to the wild-type enzyme. The formation of pyruvate is strongly inhibited by the binding of benzimidazole to E(A−A). Upon reaction with L-Ser and in the presence of the α-site substrate analogue, α-glycerol phosphate, the $Na^+$ form of βD305A undergoes inactivation via reaction of nascent α-aminoacrylate with bound PLP. This work establishes important roles for βAsp 305 both in the conformational change between open and closed states that takes place at the β-site during the formation of the E(A−A) and in substrate binding and recognition.

Substrate channeling in the tryptophan synthase bienzyme complex is regulated by allosteric interactions transmitted between the α- and β-sites. These allosteric signals are triggered by covalent bonding changes in the reacting substrate at the β-site and ligand-binding interactions at the α-site (*1*−*6*). Signal transmission occurs via a scaffolding of structural elements that includes the $Na^+/K^+/Cs^+$ monovalent cation (MVC)[1]-binding site (*7*−*12*), a network of interconnecting salt bridges (*10*−*14*), and the loops that fold down over the α-site (*2*, *15*, *16*). This signaling modulates the activities of the α- and β-subunits, and switches the α- and β-sites between open and closed conformations (*2*, *6*, *14*, *15*).

The bacterial tryptophan synthase $\alpha_2\beta_2$ complex is a bifunctional enzyme that catalyzes the last two steps in the biosynthesis of L-tryptophan (*17*−*19*) (eqs 1−3). The α-subunit catalytic site carries out the cleavage of IGP to indole and G3P (α-reaction). The β-subunit catalytic site requires the cofactor pyridoxal 5′-phosphate (PLP) that mediates the condensation between L-Ser and indole to produce L-Trp (β-reaction, Scheme 1).

The two sites are connected by a 25 Å long hydrophobic tunnel (*20*) that provides the preferred route for the transfer of the common intermediate, indole, from the α-site to the β site, preventing its escape into solution (*1*−*6*, *15*, *21*). The indole derived from IGP cleavage at the α-site reacts with L-Ser at the β site to produce L-Trp (αβ-reaction).

$$\text{IGP} \rightleftharpoons \text{G3P} + \text{indole (α-reaction)} \quad (1)$$

$$\text{Indole} + \text{L-Ser} \rightleftharpoons \text{L-Trp} + H_2O \text{ (β-reaction)} \quad (2)$$

$$\text{IGP} + \text{L-Ser} \rightleftharpoons \text{L-Trp} + \text{G3P} + H_2O \text{ (αβ-reaction)} \quad (3)$$

The overall αβ-reaction involves allosteric interactions that accomplish the coupling of the α- and β-reactions, ensuring

† Supported by NIH Grant GM55749.

* To whom correspondence should be addressed. Phone: (909) 787-4235. Fax: (909) 787-4434. E-mail: dunn@ucrac1.ucr.edu

‡ Present address: Istituto di Scienze Biochimiche, Universitá di Parma, 43100 Parma, Italy.

§ Department of Biochemistry.

|| The National Institutes of Health.

⊥ Present Address: Laboratory of Cellular and Molecular Biology, National Cancer Institute, Building 37/Room 1E24, Bethesda, MD 20892-4255.

[1] Abbreviations: $\alpha_2\beta_2$, native form of tryptophan synthase from *Salmonella typhimurium;* α, the α subunit; β, the β subunit; βD305A, the mutant in which aspartate 305 of the beta subunit has been replaced by alanine; E(Ain), the internal aldimine (Schiff base); $E(Aex_1)$, aldimine intermediates formed between the PLP cofactor and the substrate amino acids; E(A−A), the α-aminoacrylate Schiff base; $E(Q_3)$, the quinonoid intermediate that accumulates during the reaction between E(A−A) and indole; $E(Aex_2)$, the L-Trp external aldimine; PLP, pyridoxal phosphate; L-Ser, L-serine; L-Trp, L-tryptophan; DIT, dihydroiso-L-tryptophan; IGP, 3-indole-D-glycerol 3′-phosphate; GP, α-glycerol-phosphate; G3P, glyceraldehyde 3-phosphate; TEA, triethanolamine; KIE, kinetic isotope effect; RSSF, rapid-scanning stopped-flow; SWSF, single-wavelength stopped-flow; $1/\tau_n$, apparent first-order rate constant of the *n*th relaxation; $A_n$, amplitude of the *n*th relaxation; MVCs, monovalent cations.

10.1021/bi002892l CCC: $20.00 
Published on Web 06/01/2001

Scheme 1. Reactants, Products, and Intermediates in the Reaction of L-Ser and Indole (the $\beta$-Reaction) Catalyzed by the Tryptophan Synthase Bienzyme Complex

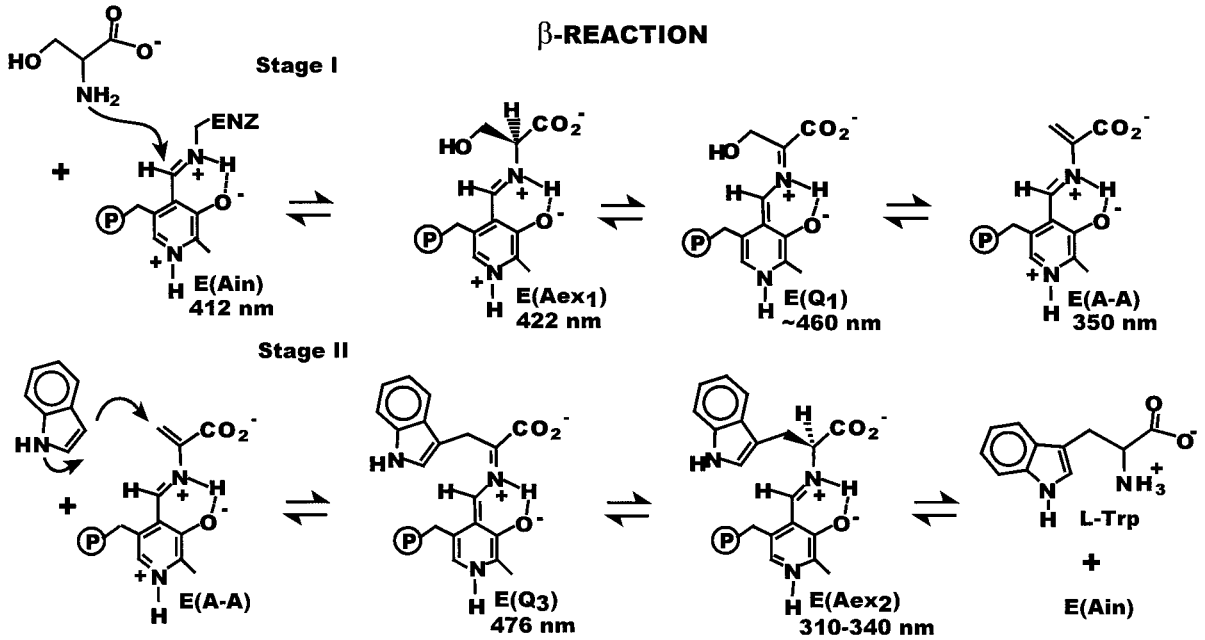


efficiency for the enzyme (*1*, *2*, *4*, *5*, *6*, *9*−*11*, *22*−*27*). This coupling is achieved by a switching of $\alpha\beta$-subunit pairs from an open and less active conformation to a closed and more active conformation that prevents the escape of indole. Formation of E(A−A) at the $\beta$-site activates the $\alpha$-site ~27-fold, while formation of E($Aex_2$) returns the $\alpha$-site to the low activity state (*2*−*4*). The binding of substrate or substrate analogues to the $\alpha$-site also generates a change in the $\beta$-reaction activity (*1*−*3*). The binding of monovalent cations (MVCs) to an allosteric site on the $\beta$-subunit strongly modulates both the catalytic activity and the integrity of these allosteric triggers (*8*−*11*).

X-ray structures have been very helpful in the identification of residues involved in the transmission of the allosteric signals. Aspartate $\beta$305 is located adjacent to the $\beta$-active site and to the metal site. The carbonyl oxygen of $\beta$F306 provides one of the MVC ligands for the $Na^+/K^+/Cs^+$ site (*12*, *16*). Asp $\beta$305 appears to occupy a pivotal position with respect to the conformational transition between open and closed states. Depending on the $\alpha$-site ligation state, the $\beta$-site covalent state, and the MVC bound to the $Na^+/K^+/Cs^+$ site, the carboxylate of $\beta$D305 forms either a salt bridge to $\beta$K167, a H-bond to the hydroxyl of the E($Aex_1$) intermediate, a salt bridge to $\beta$R141, or is exposed to solvent. The interaction between $\beta$D305 and $\beta$R141 appears to lock the $\beta$-subunit into a conformation that blocks the entrance of the $\beta$-site and, therefore, appears to play a critically important role in regulating access to and from the $\beta$-site. Consequently, Asp $\beta$305 is part of the salt bridge-switching relay that involves Asp $\alpha$56−Lys $\beta$167, Lys $\beta$167−Asp $\beta$305, and Asp $\beta$305−Arg $\beta$141. This system of alternating salt bridges links the $\alpha$ and $\beta$ sites, and is believed to form part of the scaffolding that transmits the allosteric signal. Although the X-ray structures show salt bridging among these residues, the fact that substitution of Asn for Asp at $\beta$305 has minor effects on the catalytic and regulatory properties of $\alpha_2\beta_2$ indicates that the Lys $\beta$167−Asp $\beta$305 and Asp $\beta$305−Arg $\beta$141 charge−charge interactions contribute very little to the energetics of the conformational transition (*13*).

The available X-ray structures show that Phe $\beta$306 assumes different conformations that depend on the size of the metal ion bound to the MVC site and the covalent state of the $\beta$-site. These conformational shifts in Phe $\beta$306 are likely to alter the position of $\beta$D305. Both the geometry of the active site and the ability of Asp $\beta$305 to form salt bridges with other residues would be affected.

To investigate the functional roles played by Asp $\beta$305, herein this residue has been converted to L-Ala by site-directed mutagenesis and the mutant enzyme has been subjected to a detailed mechanistic investigation. It will be shown that the smaller size and hydrophobic properties of the Ala side chain cause drastic changes in the catalytic behavior and substrate specificity of tryptophan synthase.

## MATERIALS AND METHODS

*Materials.* L-Ser, benzimidazole, indole, and GP were purchased from Sigma. Phenylhydrazine, methoxylamine, *N*-methylhydroxylamine, indoline, 2,3 diamino propionic acid, and triethanolamine were purchased from Aldrich. Aniline was purchased from Mallinckrodt and [$\alpha$-$^2$H]L-Ser from Cambridge Isotope Laboratories. Indoline was purified as previously described (*9*). IGP was synthesized as previously described (*28*). After lyophylization, the remaining $NH_4^+$ ions were removed using an A-25 anion exchange column in the $H^+$-form. Metal-free $\alpha$-glycerol-phosphate (GP) was prepared from the disodium salt by repetitively running a solution of this compound over an ion-exchange column in the $H^+$-form.

Purification of wild-type and mutant forms of the tryptophan synthase from *Salmonella typhimurium* was performed as previously described (*29*). The $\beta$D305A mutant was prepared using the expression vector pEBA-10 as the template for quick and convenient mutagenesis by megaprimer PCR (*30*), using the D305A primer 5′-A CGC ATG CTG

CGG CCC AAC GGA CGG GAA AGC GAG CCC GGC G-3′ (which contains an *Sph*I restriction site, GC ATG C) and the primer PE7 (*30*) (which contains an *Bgl*II restriction site) for one round of PCR catalyzed by Pfu DNA polymerase. The PCR fragment was purified and blunt-end inserted into the linearized pGEM-5zf(+) vector (Promega). The linearized pGEM-5zf(+) was prepared by digestion with EcoRV to produce blunt-ends, and was dephosphorylated with alkaline phosphatase to suppress self-ligation and circularization. After confirmation of the mutation by DNA sequencing, the inserted DNA fragment was liberated with *Bgl*II and *Sph*I and then ligated into the original parent plasmid (pEBA-10) which had also been digested with *Bgl*II and *Sph*I. Growth of the *Escherichia coli* host strain CB149 (*28*) harboring the mutant forms of plasmid pEBA-10 that express the *S typhimurium* tryptophan synthase $\alpha_2\beta_2$ complex and purification of the mutant $\alpha_2\beta_2$ complex were as described (*29*−*31*). Enzyme preparations were dialyzed against metal-free TEA buffer at pH 7.8 to remove any monovalent metal ions and stored in the same buffer. All the reactions were performed at 25 ± 2° C in 50 mM triethanolamine (TEA) buffer adjusted to 7.8 with HCl.

*UV*−*Vis Absorbance Measurements.* Static UV−vis absorbance spectra and activity measurements were performed on a Hewlett-Packard 8452A diode array spectrophotometer at 25 ± 2° C in 50 mM, pH 7.8, TEA buffer. To measure the activity of the α-, *β*-, and α*β*-reactions, the absorbance at 290 nm was recorded after mixing the enzyme with the appropriate substrates and effectors. The α-reaction was followed measuring the decrease in absorbance due to the cleavage of IGP to indole and G3P ($\Delta\epsilon = -1.39$ mM$^{-1}$ cm$^{-1}$) (*32*). The *β*-reaction was followed measuring the increase in absorbance due to the conversion of indole to L-Trp ($\Delta\epsilon = 1.89$ mM$^{-1}$ cm$^{-1}$). The overall α*β*-reaction was followed measuring the increase in absorbance due to the conversion of IGP to L-Trp ($\Delta\epsilon = 0.56$ mM$^{-1}$ cm$^{-1}$).

The *β*-activity for the reactions with the indole substrate analogues, indoline, and aniline, was measured by following the absorbance change at 302 nm using either $\Delta\epsilon = 1.5$ mM$^{-1}$ cm$^{-1}$ or $\Delta\epsilon = 1.0$ mM$^{-1}$ cm$^{-1}$ for the indoline and aniline reactions, respectively. Corrections were made for the production of pyruvate by following the absorbance time courses at both 340 and 350 nm.

*UV*−*Vis Titration Studies.* Titrations of the wild-type and *β*D305A mutant enzymes with L-Ser were performed to determine the apparent dissociation constants for the L-Ser reaction. Measurements were carried out in the presence of benzimidazole (BZI) to inhibit the production of pyruvate (an unwanted side reaction) and also to stabilize E(A−A) as the complex with BZI at 25 ± 2° C in 50 mM pH TEA buffer. The appearance of the E(A−A) species was followed at 350 nm.

Plots of the titration data were fitted to the following equation: $A = [\text{L-Ser}](A_\infty - A_0)/(K_{D,app} + [\text{L-Ser}])$, where $A$ is the observed absorbance, $A_\infty$ is the absorbance value extrapolated to infinite [L-Ser], and $A_0$ is the absorbance at time zero. Since the appearance of E(A−A) involves both binding and chemical steps, the measured values gave apparent dissociation constants, $K_{D,app}$. The same method was used to investigate MVC effects.

*Rapid-Scanning Stopped-Flow and Single-Wavelength Stopped-Flow Measurements.* RSSF and SWSF measurements were performed as previously described at 25 ± 2° C in 50 mM, pH 7.8, TEA buffer (*33*−*37*). In each RSSF experiment, a set of 25 scans was collected. Two different timing sequences were used. Timing sequence 1: (1) = 8.54 ms, (2) = 17.09 ms, (3) = 25.63 ms, (4) = 34.18 ms, (5) = 42.72 ms, (6) = 59.81 ms, (8) = 93.98 ms, (10) = 0.1282 s, (15) = 0.3845 s, (20) = 0.8544 s, (25) = 1.7088 s. Timing sequence 2: (1) = 8.54 ms, (2) = 17.09 ms, (3) = 25.63 ms, (4) = 34.18 ms, (5) = 42.72 ms, (6) = 76.90 ms, (8) = 0.1452 s, (10) = 0.2136 s, (15) = 0.6408 s, (20) = 1.7088 s, (25) = 4.2720 s.

The rapid formation and decay of E(Aex$_1$) was followed by measuring the envelope of fluorescence emission provided by cutoff filters ($\lambda_{ex} = 420$ nm) (*35*). The fluorescence time courses were fitted by nonlinear least-squares regression analysis to a sum of exponentials according to the following eq 38:

$$F_t = F_\infty + \sum_i F_i \exp(-t/\tau_i)$$

where $F_t$ is the fluorescence at time $t$, $F_\infty$ is the final fluorescence, $F_i$ is the fluorescence due to the $i$th relaxation, and $1/\tau_i$ corresponds to the observed rate for the $i$th relaxation.

Analysis of stopped-flow fluorescence and UV−vis absorption time courses were performed using the software Peakfit (version 4, Jandel Scientific) and Sigmaplot (version 4, SPSS).

## RESULTS

To explore the effects of the *β*D305A mutation, UV−vis spectroscopy and rapid kinetic measurements were performed to investigate the altered catalytic behavior of the mutant. Reactions at the α- and *β*-sites with and without MVCs and the α-subunit-specific ligand GP were compared with the behavior of the wild-type enzyme. Static and kinetic UV−vis spectroscopy was also utilized to monitor the reaction of *β*D305A with L-Ser and with various nucleophilic analogues of indole to produce new L-amino acids.

*Static UV*−*Vis Absorbance Measurements. (i) Pyruvate Formation.* The reaction of *β*D305A with 40 mM L-Ser was followed for 20 m, either without allosteric effector or in the presence of 50 mM $NH_4^+$ or 100 mM $Cs^+$ at pH 7.8. Under these conditions, there is a large increase in absorbance in the 320 nm region during reaction (Figure 1). These spectral changes result from a remarkably high rate of production of pyruvate, the consequence of a well-known tryptophan synthase side reaction (see Scheme 2). The corresponding reaction in the wild-type enzyme is 15-fold slower under the same conditions.

*(ii) Covalent Inactivation.* In the presence of GP alone, or with GP and MVCs, the mutant enzyme undergoes inactivation and the PLP absorbance at 412 nm disappears (Figure 1). The same behavior, but on a slower time scale, is seen in the presence of NaCl. At the end of the reaction, shifting the pH to a value of 13, gives a spectrum with an absorption band at 424 nm. This spectral change is characteristic of a chemical reaction that was first proposed for the mechanism-based inactivation of aspartate aminotransferase and glutamate decarboxylase (*39*, *40*) (Scheme 2C).

Scheme 2. Reaction Schemes Showing Proposed Mechanisms for the Formation of Pyruvate from the E(A−A) Intermediate (A and B), and the Proposed Pathway for the Covalent Reaction of α-Aminoacrylate with E(Ain) (C)

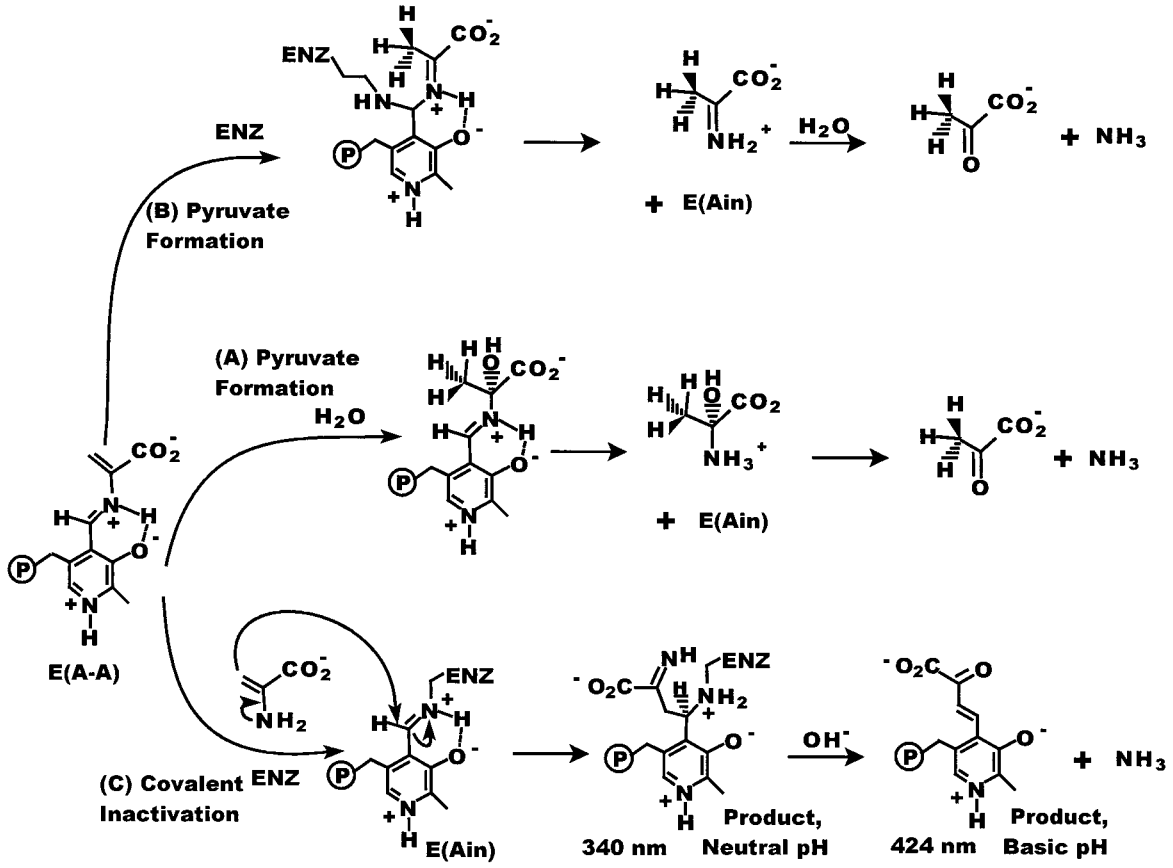


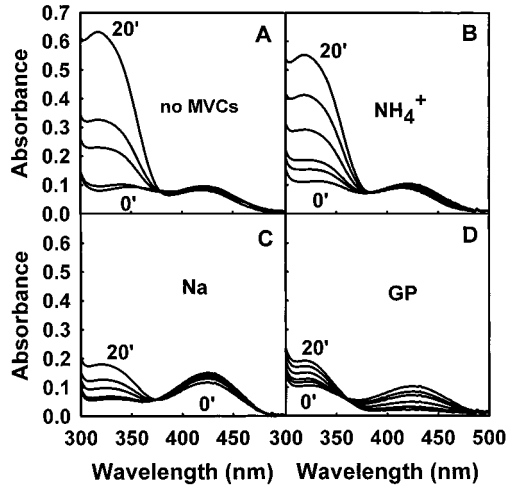


FIGURE 1: Spectra showing the changes that occur during the reaction of 10 $\mu$M $\beta$D305A ($\alpha_2\beta_2$) mutant enzyme with 40 mM L-Ser (A), in the presence of 50 mM $NH_4Cl$ (B); 100 mM NaCl (C); or 50 mM GP (D). Reaction was followed for 20 m with spectra recorded at 0, 1, 3, 5, 10, and 20 m. Spectra were measured at 25 ± 2° C in 50 mM, pH 7.8, TEA buffer.

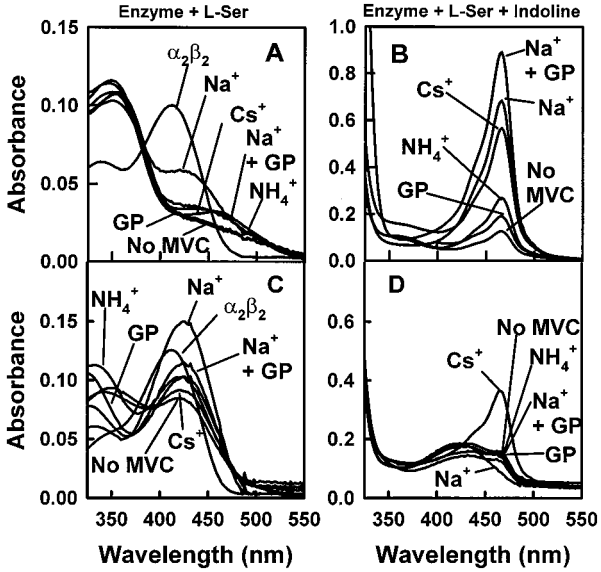


FIGURE 2: Static UV−vis spectra comparing the reaction of wild-type and $\beta$D305A mutant enzymes (each 7 $\mu$M $\alpha_2\beta_2$) with 40 mM L-Ser (A, C) and 4.5 mM indoline (B, D). The reactions were performed in the absence of effectors, and in the presence of 100 mM NaCl; 50 mM $NH_4Cl$; 50 mM GP; 100 mM NaCl and 50 mM GP; or 100 mM CsCl, all at 25 ± 2° C in 50 mM, pH 7.8, TEA buffer. Spectrum $\alpha_2\beta_2$: 7 $\mu$M $\beta$D305A or wild-type mutant enzyme in buffer.

This type of inactivation has also been demonstrated for several mutant forms of tryptophan synthase including $\beta$D305N and $\beta$S377D (*41*, *42*).

*(iii) Time-Resolved Spectra.* In Figure 2 the spectral changes that occur with and without allosteric effector are shown, both in the reaction of the $\beta$D305A mutant with L-Ser (panel C) and in the reaction with L-Ser and indoline (panel D). To avoid absorbance contributions due to the formation of pyruvate, L-Ser was added at the last moment and spectra were recorded within a few seconds after mixing. Figure 2 also shows the same reactions for the wild-type enzyme (panels A and B).

Table 1[a]

| | reaction activity ($s^{-1}$) | | | | | | | |
|---|---|---|---|---|---|---|---|---|
| | α | | β | | αβ | | αβ/α | |
| effectors | wild-type | βD305A | wild-type | βD305A | wild-type | βD305A | wild-type | βD305A |
| none | 0.3 | 0.44 | 1.6 | 0.88 | 0.3 | 0.3 | 1 | 0.7 |
| $Na^+$ | 0.1 | 0.30 | 7.4 | 0.40 | 3 | 0.04 | 30 | 0.1 |
| $K^+$ | 0.1 | 0.28 | 11 | 0.80 | 2.6 | 0.28 | 26 | 1 |
| $NH_4^+$ | 0.05 | 0.30 | 13 | 5.0 | 2 | 2.9 | 40 | 9 |
| $Cs^+$ | 0.07 | 0.30 | 14 | 7.8 | 3.8 | 3.1 | 54 | 10 |
| GP | | | 0.4 | 0.54 | | | | |
| $Na^+$ + GP | | | 2.9 | 0.56 | | | | |
| $NH_4^+$ + GP | | | 1.4 | 1.6 | | | | |

[a] Reaction conditions: [enzyme] = 0.5 μM; α-reaction: [IGP] = 0.2 mM. β-reaction: [L-Ser] = 40 mM, [indole] = 0.2 mM. αβ-reaction: [L-Ser] = 40 mM, [IGP] = 0.2 mM. Effector concentrations: [NaCl] = 100 mM; [KCl] = 100 mM; [$NH_4Cl$] = 50 mM; [CsCl] = 100 mM; [GP] = 50 mM. All reactions were measured at 25 ± 2° C in 50 mM, pH 7.8, TEA buffer. Error limits were estimated to be ±10%.

The distributions of intermediates formed at equilibrium are significantly different from those of the wild-type enzyme. In the wild-type system, the presence of $Cs^+$, $NH_4^+$, GP, GP plus $Na^+$, or without effectors drives the distribution in favor of E(A−A), while $Na^+$ gives comparable amounts of E($Aex_1$) and E(A−A) (*8*−*10*, *13*, *43*). In the βD305A mutant, L-Ser reacts in the presence of $Cs^+$, $NH_4^+$, GP, GP plus $Na^+$, or without effectors, to give a distribution consisting of comparable amounts of E(A−A) and E($Aex_1$), while $Na^+$ shifts the equilibrium strongly in favor of E($Aex_1$).

The reaction of wild-type enzyme with L-Ser and the analogue indoline gives a quasi-stable quinonoid, $E(Q)_{indoline}$, resulting from the nucleophilic attack of the indoline N-1 on the β-C of the E(A−A) intermediate. In the wild-type system, this quinonoid is strongly stabilized by $Na^+$ or the combination of $Na^+$ and GP, while in the absence of MVCs, in the presence of $NH_4^+$, or in the presence of MVC-free GP, the predominating species is E(A−A) (*9*−*11*, *13*). The accumulation of $E(Q)_{indoline}$ is greatly impaired in the βD305A mutant; only $Cs^+$ gives a substantial amount of $E(Q)_{indoline}$, $Na^+$ gives no detectable amount of quinonoid, and all the other effectors give only small amounts of the quinonoid.

*Steady-State Activities for the Reactions Catalyzed by the Wild-Type and βD305A Bienzyme Complexes.* Table 1 summarizes the rates for the reactions of IGP (α reaction), L-Ser plus indole (β reaction) and L-Ser plus IGP (αβ reaction) with the mutant and with the wild-type enzyme. The rate of the α-subunit-catalyzed cleavage of IGP to indole and G3P is slightly greater for the mutant than for the wild-type enzyme, and the rates are essentially unaffected by the MVCs.

The mutation does not affect the rate of the αβ-reaction in the absence of effectors (Table 1). $Na^+$ strongly inhibits this reaction, whereas the $K^+$ form shows the same activity seen in the MVC-free mutant (a value that is 10-fold less than the activity of the wild-type $K^+$ form). Both $NH_4^+$ and $Cs^+$ show a significant activation of the mutant enzyme system that brings the rate of production of L-Trp to the level of the wild-type enzyme reaction.

In the absence of MVCs and GP, the β activity is 55% of the wild-type form. Again, $Na^+$ inhibits, $K^+$ does not show any remarkable effect, and $NH_4^+$ or $Cs^+$ stimulate. These data establish that, as the MVC size increases, the rate of the β reaction also increases for both wild-type and βD305A mutant enzymes.

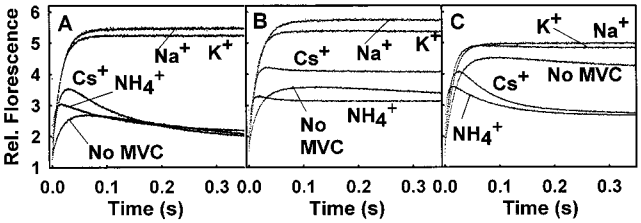


FIGURE 3: Fluorescence stopped-flow time courses are shown for the reactions of 10 μM $\alpha_2\beta_2$ βD305A mutant in one syringe and 40 mM L-Ser (A); 40 mM L-Ser and 0.5 mM indole (B); or 40 mM L-Ser and 0.5 mM IGP (C) in the other syringe. Conditions: [NaCl] = 100 mM; [KCl] = 100 mM; [$NH_4Cl$] = 50 mM; [CsCl] = 100 mM, at 25 ± 2° C in 50 mM, pH 7.8, TEA buffer. Identical MVC concentrations were loaded in each syringe.

The data in Table 1 show that both GP binding and the combination of $Na^+$ and GP suppress the activity of the mutant enzyme. These activities likely are influenced by both the allosteric effects of $Na^+$ and GP and by the covalent inactivation of the enzyme. The ratio of the αβ/α activities (Table 1) shows that L-Ser bound to the β-site of the mutant enzyme stimulates the rate of the α-reaction only in the presence of $NH_4^+$ and $Cs^+$. The MVC-free and the $Na^+$ forms exhibit a ratio of the αβ to α activities (αβ/α) less than 1, while the wild-type enzyme gives a value of ∼27 (*3*, *4*). This ratio measures the activation of the α-site by L-Ser reaction at the β-site.

*Stopped-Flow Fluorescence Measurements.* The E($Aex_1$) intermediate is the only species in the tryptophan synthase pathway that gives a strong fluorescence signal. Using a 420 nm excitation wavelength, the fluorescence emission signal provides an uncomplicated measure of the formation and decay of E($Aex_1$) (Figure 3). Table 2 shows the relaxation rate constants and amplitudes for the formation and decay of the E($Aex_1$) species in the following reactions: stage I of the β-reaction (reaction of L-Ser), the β-reaction (reaction of L-Ser plus indole), the αβ-reaction (reaction of L-Ser plus IGP) both for the wild-type and for the βD305A mutant forms of tryptophan synthase.

In the reaction with L-Ser in the presence of $Na^+$ or $K^+$, the βD305A system gives rates for the formation of E($Aex_1$) that are much slower than those of the wild-type enzyme, and unlike the wild-type system, no decay is detected. Without MVCs and in the presence of $NH_4^+$ or $Cs^+$, a slow decay phase is seen. $NH_4^+$ shows the fastest rate of E($Aex_1$) formation, whereas $Cs^+$ shows the fastest rate of decay.

Table 2[a]

Tryptophan Synthase + L-Serine (stage I of the $\beta$-reaction)

| | no MVCs | | $Na^+$ | | $K^+$ | | $NH_4^+$ | | $Cs^+$ | |
|---|---|---|---|---|---|---|---|---|---|---|
| $1/\tau$ ($s^{-1}$) | WT | $\beta$D305A | WT | $\beta$D305A | WT | $\beta$D305A | WT | $\beta$D305A | WT | $\beta$D305A |
| $1/\tau_1$ (up) | 200 | 60 | 900 | 60 | 660 | 60 | 420 | 240 | 250 | 100 |
| $1/\tau_2$ (up) | | | 50−100 | | | | | | | |
| $1/\tau_3$ (down) | 21 | 1.7 | 7 | | 20 | | 90 | 7.6 | 70 | 8.0 |
| $A_1/A_2$ or $A_3$ | | 0.8 | | | 0.5 | | 0.7 | 1.3 | 0.6 | 1.2 |

Tryptophan Synthase + L-Serine + Indole (the Overall $\beta$-reaction)

| | no MVCs | | $Na^+$ | | $K^+$ | | $NH_4^+$ | | $Cs^+$ | |
|---|---|---|---|---|---|---|---|---|---|---|
| $1/\tau$ ($s^{-1}$) | WT | $\beta$D305A | WT | $\beta$D305A | WT | $\beta$D305A | WT | $\beta$D305A | WT | $\beta$D305A |
| $1/\tau_1$ (up) | 210 | 46 | 900 | 53 | 600 | 70 | 350 | 250 | 200 | 120 |
| $1/\tau_2$ (up) | | | 50−100 | | | | | | | |
| $1/\tau_3$ (down) | 0.5 | | | | 30 | | 100 | 30 | 85 | 20 |
| $A_1/A_2$ or $A_3$ | 1 | | | | 0.6 | | 0.8 | 5.2 | 0.8 | 7.4 |

Tryptophan Synthase + L-Serine + IGP (the $\alpha\beta$-reaction)

| | no MVCs | | $Na^+$ | | $K^+$ | | $NH_4^+$ | | $Cs^+$ | |
|---|---|---|---|---|---|---|---|---|---|---|
| $1/\tau$ ($s^{-1}$) | WT | $\beta$D305A | WT | $\beta$D305A | WT | $\beta$D305A | WT | $\beta$D305A | WT | $\beta$D305A |
| $1/\tau_1$ (up) | 250 | 52 | 650 | 64 | 680 | 80 | 480 | 260 | 350 | 120 |
| $1/\tau_2$ (down) | 25 | 0.6 | 20 | | 25 | 0.2 | 85 | 10 | 70 | 15 |
| $A_1/A_2$ | 0.8 | 1.6 | 0.5 | | 0.4 | 2.1 | 0.6 | 1.5 | 0.6 | 1.5 |

[a] Relaxation rate constants and amplitudes are taken from data collected under the conditions shown in Figure 3. Rates calculated from increasing fluorescence are indicated as (up), rates calculated from decreasing fluorescence are indicated as (down). Error limits are estimated to be ±15%.

When L-Ser and indole are mixed with the enzyme, the rates for the formation of $E(Aex_1)$ are not affected by the presence of indole in either the mutant or the wild-type enzyme. The presence of indole and $NH_4^+$ or $Cs^+$ increases the decay rate by 3-fold. Without MVCs or in the presence of $Na^+$, no decay phase is seen for either the $\beta$D305A mutant or the wild-type enzyme.

In the reactions with L-Ser and IGP, again the rates of $E(Aex_1)$ formation are very similar to the rates obtained with L-Ser alone. The reaction of wild-type enzyme with IGP exhibits large amplitudes for the decay phase, both in the presence of $Na^+$ and in the absence of MVCs. Under the same conditions, the mutant system does not show a decay process. With IGP, the $K^+$ form of the mutant enzyme shows a very slow decay phase that was not detected in the reaction of the $K^+$ form with either L-Ser or with L-Ser and indole.

*Rapid Scanning Stopped-Flow Studies (data not shown).* The reaction of $\beta$D305A with L-Ser in the presence of $NH_4^+$, $Cs^+$, or without MVCs exhibits a rapid formation of $E(Aex_1)$. With $NH_4^+$, the decay phase yields an equilibrium mixture dominated by $E(Aex_1)$ and E(A−A). In the presence of $K^+$, the $E(Aex_1)$ species is stabilized, and the system undergoes no further reaction.

Reaction of IGP with the $NH_4^+$-, $Cs^+$-, and MVCs-free forms of the mutant enzyme gives time courses for the formation and decay of $E(Aex_1)$ that are unaffected by the presence of substrate in the α-site. $K^+$ stabilizes the $E(Aex_1)$ species. The RSSF spectra are in agreement with the results obtained in the stopped-flow fluorescence measurements (see Figure 3).

*Kinetic Isotopic Effects for C-α Deprotonation.* Deuterium isotope effects resulting from the substitution of $^2H$ for $^1H$ at C-α of L-Ser in the $\beta$-reaction were determined for the $\beta$D305A mutant enzyme. The results are summarized and compared with data for the wild-type enzyme in Table 3. In the mutant enzyme system, the MVC-free form has the smallest KIE (3.1), whereas the MVC-bound forms show larger isotopic effects ranging from 5.0 to 6.2. The wild-type enzyme exhibits significant KIEs only with $Na^+$ and $K^+$ (respectively 5.0 and 3.0).

Table 3: Primary Kinetic Isotope Effects for the $\beta$-reaction Activities of Wild-Type and $\beta$D305A Mutant Enzyme[a]

| | activities ($s^{-1}$) | | | | | |
|---|---|---|---|---|---|---|
| | wild-type | | | $\beta$D305A | | |
| effectors | L-Ser | α-$^2$H-L-Ser | KIE | L-Ser | α-$^2$H-L-Ser | KIE |
| none | 2.0 | 1.8 | 1.1 | 0.88 | 0.28 | 3.1 |
| $Na^+$ | 8.0 | 1.5 | 5.3 | 0.40 | 0.08 | 5.0 |
| $K^+$ | 12 | 4 | 3 | 0.80 | 0.14 | 5.7 |
| $NH_4^+$ | 10.3 | 7.9 | 1.2 | 5.0 | 0.8 | 6.2 |
| $Cs^+$ | 14 | | | 7.8 | 1.8 | 4.3 |

[a] Conditions for the reactions: [enzyme] = 0.5 $\mu$M, [L-Ser or α-$^2$H-L-Ser] = 40 mM, [indole] = 0.2 mM. Effector concentrations: [NaCl] = 100 mM; [KCl] = 100 mM; [$NH_4Cl$] = 50 mM; [CsCl] = 100 mM; or [GP] = 50 mM, all at 25 ± 2° C in 50 mM, pH 7.8, TEA buffer. Error limits were estimated to be ±10%.

*Reaction of the D305A Mutant with Indole Analogues and Other Nucleophiles in the Presence of CsCl.* Since $Cs^+$ was found to give the largest effect, both on the $\beta$-activity and on E(Q) stabilization in the $\beta$D305A mutant system, all of the analogue investigations described below were performed in the presence of 100 mM CsCl. Figure 4 shows UV−vis spectra collected during the reactions of the wild-type and the D305A mutant enzymes with L-Ser and with various nucleophiles in the presence of 100 mM $Cs^+$ for a period of 30 m.

*(i) Benzimidazole (BZI).* Reaction of this indole analogue in the wild-type system has been previously studied (*1*, *2*, *44*). This compound binds (and stabilizes) but does not react covalently with the E(A−A) species. BZI also binds to the E(A−A) form of the D305A mutant. Formation of the BZI complex almost completely inhibits the production of pyruvate (Figure 4, panels A and B).

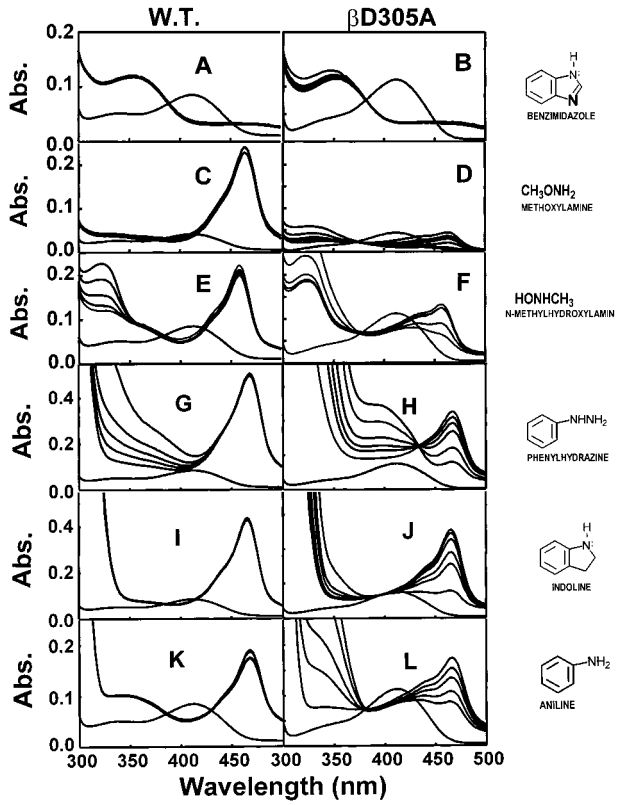


FIGURE 4: Spectra comparing the changes that occur during the reaction of wild-type and $\beta$D305A mutant enzymes with L-Ser 40 mM and 5 mM benzimidazole (A, B); 5 mM methoxylamine (C, D); 5 mM *N*-methylhydroxylamine (E, F); 5 mM phenylhydrazine (G, H); 5 mM indoline (I, J), or 5 mM aniline (K, L) all in the presence of 100 mM CsCl, all at 25 ± 2° C in 50 mM, pH 7.8, TEA buffer. Enzyme concentrations are 5−10 $\mu$M. Reactions were followed for 30 m. Spectra were taken at 0, 1, 3, 5, 10, and 30 m.

*(ii) Indoline.* The reaction of the wild-type enzyme with L-Ser and indoline to produce the new amino acid, dihydroiso-L-tryptophan (DIT), has been extensively studied (*2*, *13*, *15*, *21*, *24*, *44*). DIT has a UV−vis spectrum that is almost identical in shape to indoline but red shifted by 10 nm.

The reaction of L-Ser and indoline both with $\beta$D305A and with the wild-type enzyme in the presence of $Cs^+$ over a 30 m interval is shown in Figures 5, panels I and J. Upon completion of reaction, DIT was purified as previously described (*44*). The UV−vis spectrum of the isolated product was found to be identical to the DIT UV−vis spectrum previously published (*44*).

Reaction of 20 mM L-Ser, 2 mM indoline, and 1 $\mu$M $\alpha_2\beta_2$ D305A mutant enzyme in the presence of 100 mM $Cs^+$ gives a value for the $\beta$-activity of 1.4 $s^{-1}$ and a yield of ~80%. This activity is only 2.7-fold lower than the value found for the natural substrate, indole, under the same conditions. In contrast, the wild-type enzyme has an activity under the same conditions that is 14-fold smaller (0.1 $s^{-1}$).

*(iii) Aniline.* The UV−vis spectra obtained for the reactions of the wild-type and the D305A mutant enzymes with L-Ser and aniline in the presence of 100 mM $Cs^+$ show remarkably different behavior. The wild-type enzyme reacts to produce a quinonoid that is stable for greater than 30 m. The amount of quinonoid formed with the mutant is comparable to the wild-type enzyme but, in this case, the quinonoid is a transient species; the spectrum taken after 1 m already shows significant decay of the quinonoid. The half-life for decay was found to be approximately 30 m (Figure 4, panels K and L).

After reaction with the mutant enzyme was complete, the product was purified using the same procedure utilized for DIT. The isolated product gave a spectrum similar to the spectrum of aniline, but red-shifted by 10. The mass spectrum for the purified sample gave a value for M + 1 = 181, a value consistent with the molecular weight expected for $\beta$-*N*-anilino-L-Ala, the anticipated product from the reaction between L-Ser and aniline.

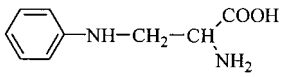


Reaction of 20 mM L-Ser with 1.5 mM aniline catalyzed by 1 $\mu$M $\alpha_2\beta_2$ D305A mutant enzyme in the presence of 100 mM $Cs^+$ gave a $\beta$-activity of 0.15 $s^{-1}$ and a yield of ~30%. Under the same conditions, the wild-type enzyme does not produce detectable amounts of $\beta$-*N*-anilino-L-Ala.

*(iv) Methoxylamine.* In the presence of L-Ser, methoxylamine (*O*-methylhydroxylamine) reacts with the wild-type enzyme to produce a quinonoid species that is stable for at least half an hour (*1*, *21*). With the $\beta$D305A mutant enzyme, the amount of quinonoid that accumulates is smaller and this transient species completely disappears after 30 m (Figure 4, panels C and D). To determine if a new amino acid is produced in this reaction, separation of the products by thin-layer chromatography (TLC) using silica gel plates detected two ninhydrin-positive compounds. One corresponds to unreacted L-Ser, and the other appears to be a new amino acid obtained from the condensation of L-Ser and methoxylamine.

*(v) N-Methylhydroxylamine.* Again, with the $\beta$D305A mutant there is less accumulation of the quinonoid species than with the wild-type enzyme, and the decay of this species is almost complete after 30 m. In the wild-type system (*1*, *21*), the amount of quinonoid formed is almost twice that in the mutant enzyme, and, after half an hour, only a small amount of decay is seen (Figure 4, panels E and F). TLC and ninhydrin staining also gave evidence for the presence of a new amino acid.

*(vi) Phenylhydrazine.* This compound reacts with the E(A−A) species of the wild-type enzyme to form a quinonoid species that is stable for 30 m (*1*, *21*). In the $\beta$D305A system, instead, there is a rapid decay of the quinonoid that is complete in 30 m (Figure 4, panels G and H). The decay of the quinonoid is accompanied by large spectral changes in the region below 430 nm. Closer investigation of the reaction shows that the spectral changes below 430 nm primarily are due to the reaction of excess phenylhydrazine with the pyruvate derived from the side reaction, giving the phenylhydrazone of pyruvate. Because this reaction dominates the UV−vis spectrum, we were unable to determine from difference spectra whether phenylhydrazine also reacts to produce the corresponding amino acid. Evidence for a new amino acid from TLC and ninhydrin staining was inconclusive.

*L-Ser Titration.* Benzimidazole stabilizes the E(A−A) species in both wild-type and D305A mutant forms of tryptophan synthase (*1*, *23*) and almost completely inhibits the production of pyruvate in the mutant enzyme. This

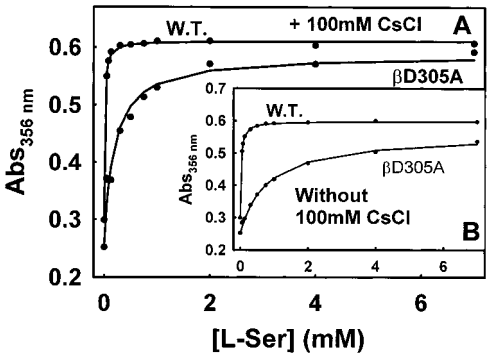


FIGURE 5: Comparison of the titrations of wild-type and $\beta$D305A mutant enzymes (each 30 $\mu$M) with L-Ser in the presence of 100 mM CsCl and 5 mM benzimidazole (A) or 5 mM benzimidazole only (B) at 25 ± 2° C in 50 mM, pH 7.8, TEA buffer. The line drawn through the data points is the best fit to the equation $A = [\text{L-Ser}](A_\infty - A_0)/(K_{D,app} + [\text{L-Ser}])$, where $A$ is the observed absorbance and $A_\infty$ and $A_0$ are the absorbance values when the [L-Ser] is ∞ and 0, respectively.

Table 4: Apparent Dissociation Constants, $K_{D,app}$, from the Titration of Wild-Type and $\beta$D305A Mutant Enzyme with L-Ser.

| enzyme | benzimidazole (mM) | CsCl (mM) | $K_{D,app}$ (mM) |
|---|---|---|---|
| wild-type | | | 0.074 |
| | | 100 | 0.044 |
| | 5 | | 0.023 |
| | 5 | 100 | 0.011 |
| $\beta$D305A | 5 | | 0.80 |
| | 5 | 100 | 0.18 |

[a] Data were collected under the conditions showed in Figure 5. The data were fitted to the equation $A = [\text{L-Ser}](A_\infty - A_0)/(K_{D,app} + [\text{L-Ser}])$, where $A$ is the absorbance and $A_\infty$ and $A_0$ are the absorbance when the [L-Ser] is ∞ and 0, respectively.

inhibition of pyruvate formation made possible the titration of D305A with L-Ser to give the benzimidazole complex of E(A−A). Figure 5 shows the titration isotherms. The $K_{D,app}$ values reported in Table 4 were calculated by fitting the titration curves with the equation $A = [\text{L-Ser}](A_\infty - A_0)/(K_{D,app} + [\text{L-Ser}])$, where $A$ is the absorbance and $A_\infty$ and $A_0$ are the absorbance values when the [L-Ser] is ∞ and 0, respectively. In the absence of MVCs, the apparent $K_{D,app}$ for the D305A mutant is almost 40 times larger than for the wild-type enzyme. After addition of 100 mM $Cs^+$, the $K_{D,app}$ value for the wild-type enzyme decreased by 2-fold, and the $K_{D,app}$ for the mutant form decreased by 4-fold.

*Reaction with the L-Ser Analogue 2,3-D,L-Diaminopropionic Acid (DAPA).* Figure 6 shows the spectral changes that occur over the first 10 m during the reactions of the wild-type and D305A mutant enzymes with DAPA. Upon reaction with 40 mM DAPA, the wild-type enzyme exhibits spectral changes characteristic of E(A−A) formation (a decrease in the 412 nm band and an increase in the 350 nm band).

Under the same conditions, the $\beta$D305A mutant enzyme, shows no spectral changes. The small increases in the absorbance at 300−350 nm present in Figure 6B are due to the free form of the L-Ser analogue. When the concentration of DAPA was increased from 40 to 200 mM, the 460−550 nm region shows changes indicating some formation of E(A−A), and the 320 nm region shows increased absorbance due to the slow formation of pyruvate. Since the absorbance at 412 nm characteristic of E(Ain) is essentially unchanged,

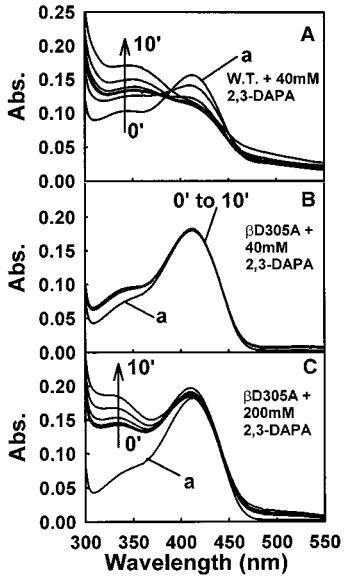


FIGURE 6: Spectra showing the changes that occur during the reaction of wild-type (A) and $\beta$D305A mutant (B) enzymes (each 10 $\mu$M $\alpha_2\beta_2$) with 40 mM 2,3-diaminopropionic acid in the presence of 100 mM CsCl, and reaction of 10 $\mu$M $\alpha_2\beta_2$ $\beta$D305A mutant enzyme with 200 mM 2,3-diaminopropionic acid in the presence of 100 mM CsCl (C) at 25 ± 2° C in 50 mM, pH 7.8, TEA buffer. Reaction was followed for 10 m. Spectra were recorded at 0, 1, 2, 5, and 10 m.

it appears that the affinity of the mutant enzyme for DAPA is very low and the fraction of enzyme sites converted to E(A−A) is small.

## DISCUSSION

*Intermediate Formation, Salt Bridging Interactions, and Subunit Conformation.* The X-ray structures of tryptophan synthase are critically important for identifying residues with potential roles in catalysis and allosteric regulation. These structures show that $\beta$D305 is placed at the junction between the $\beta$ active site and the MVC site (Figure 7A). In the refined structure of the $Na^+$ form of E(Ain) (PDB file 1BKS), the side chain of $\beta$K167 is assigned two orientations, one gives a salt bridge with $\beta$D305, the other with αD56. In the latter conformation, the side chain of $\beta$D305 is rotated to an alternative position where it makes no bonding interactions with the protein, but, instead, is solvent exposed and H-bonded to a water molecule. In the $K^+$ and $Cs^+$ forms of E(Ain), $\beta$K167 forms salt bridging interactions with αD56, and again $\beta$D305 is solvent exposed. The structure of the $Na^+$ complex of E($Aex_1$) formed with the $\beta$K87T mutant (PDB file 1UBS) (*16*) reveals that the carboxylate of $\beta$D305 is located within H-bonding distance of the hydroxyl group of the bound L-Ser moiety. The $\beta$-site appears only partially closed in this structure, while the α-subunit has the open conformation. In the structures of the $Na^+$ forms of E($Aex_1$) with either IPP (file 2TRS) (*16*) or GP (PDB file 2TSY) (*16*) bound to the α-site, $\beta$D305 forms salt bridges with $\beta$R141, and the conformations of the α- and $\beta$-subunits are closed. The $Na^+$ form of E($Aex_2$) (PDB file 2TYS) (*16*) shows a salt bridge between $\beta$D305 and $\beta$R141, and the $\beta$-subunit conformation appears to be closed. Thus, formation of the $\beta$D305-$\beta$R141 salt bridge blocks entry into the $\beta$-site and appears critically important for the transition to the closed conformation.

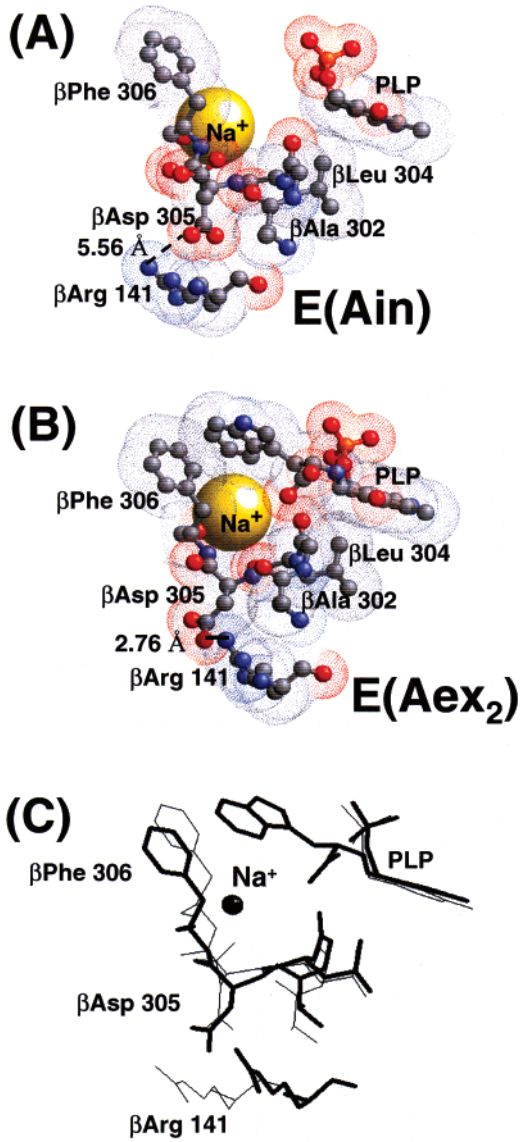


FIGURE 7: Comparison of $\beta$-site structural details for the internal aldimine (A), E(Ain), and the L-Trp external aldimine (B), E(Aex$_2$) formed with the $\beta$K87T mutant. The superimposed sites are shown in (C). The structures shown in panels (A) and (B) consist of the pyridoxal phosphate ring system (PLP, in CPK colors), $\beta$-site amino acid residues 302−306 and $\beta$Arg 141 (shown as ball-and-sticks in CPK colors), and $Na^+$ (yellow ball) bound to the monovalent cation site. The distances separating the carboxylate of $\beta$D305 and the guanidium group of $\beta$R161 are also shown. Panel C presents the superimposed structures with E(Ain) in thin black wireframe, E(Aex$_2$) in thick black wireframe, and $Na^+$ as a black ball. In the closed structure of E(Aex$_2$) (B), $\beta$Asp 305 and $\beta$Arg 141 form a H-bonded salt bridge (black line), and the indole ring of E(Aex$_2$) makes van der Waals contact with the ring of $\beta$Phe 306. In the open structure of E(Ain), $\beta$Asp 305 and $\beta$Arg 141 are too far apart to form a salt bridge. The superimposed structures (C) show that the $\beta$Phe 306 ring is displaced upon formation of E(Aex$_2$). The two structures were superimposed by aligning as closely as possible the $Na^+$ ions and the $\alpha$-subunits (not shown) of the two structures. The E(Ain) structure was taken from PDB file 1BKS, the E(Aex$_2$) structure was taken from PDB file 2TYS (*16*).

Salt bridging between $\beta$D305 and $\beta$R141 with H-bonding between the Asp carboxylate and the Arg guanidinium group is found in essentially all of the structures with closed or partially closed $\beta$-subunit conformations (Figure 7B). This salt bridge does not occur in the $Na^+$-form of E(Ain) (the open conformation, PDB file 1BKS), indeed, the two side chain termini are oriented in opposite directions and separated by 5.56 Å (Figure 7A). In the $K^+$ and $Cs^+$ forms of E(Ain) (PDB files 1TTQ and 1TTP) (*12*), these side chains are separated by 11.2 and 13.2 Å, respectively, and the protein has the open conformation. In structures where the $\alpha$-site has a bound ligand and a closed conformation, and the $\beta$-site has an open conformation (PDB files 1A5O, 1C29, 1C8V, 1C9D, 1CW2) (*45, 46*), the $\beta$D305 carboxylate and the $\beta$R141 guanidium group are typically 5.3−6.45 Å apart. Thus, the formation of the salt bridge between $\beta$D305 and $\beta$R141 appears to coincide with, and be obligatory for, the conversion of the $\beta$-subunit from the open to the closed conformation.

The carbonyl oxygen of $\beta$Phe 306, the residue following $\beta$Asp 305, provides one of the ligands for the monovalent cation metal site (*12*). The flat hydrophobic surface of the aromatic ring of this side chain likely makes van der Waals contact with the indole ring during the reaction of indole with the E(A−A). As shown in Figure 7B, this interaction occurs in the structure of the E(Aex$_2$) intermediate formed with the K87T mutant (PDB code 2TYS) (*12*).

*Mechanistic Implications of Pyruvate Formation.* In the absence of MVCs and in the presence of $NH_4^+$ or $Cs^+$ (data not shown), the reaction of the $\beta$D305A mutant with L-Ser gives spectral changes that are dominated by the production of pyruvate (Figure 1). In contrast, when the wild-type enzyme reacts under the same conditions, only traces of pyruvate are detected.

The formation of pyruvate has its origins in a tryptophan synthase side reaction that involves deamination of the $\alpha$-aminoacrylate Schiff base to pyruvate and ammonia (*47, 48*). Scheme 2, mechanisms A and B, show two possible mechanisms for pyruvate formation that are consistent with the finding of Tsai et al. (*47*) that a hydrogen is stereospecifically transferred to the C-3 of pyruvate in the tryptophan synthase $\beta_2$-mediated conversion of L-Ser to pyruvate. This finding implies the proton transfer to the C-3 methyl group occurs while it is still attached to the enzyme (*48*). In mechanism A, water adds across the aminoacrylate double bond to generate the methyl group and form a tetrahedral adduct at C-$\alpha$. Then $\beta$Lys 87 attacks the Schiff base linkage of the tetrahedral adduct, the adduct is released, and then converted to pyruvate and ammonia. In mechanism B, $\beta$Lys 87 makes a nucleophilic attack on the E(A−A) Schiff base linkage to form a gem diamine at C-4′ as a proton is added to C-$\beta$. This pyruvate ketimine is then transformed to E(Ain) and the imine of pyruvate. Hydrolysis of the protonated pyruvate imine in solution then yields pyruvate and ammonia. Assuming that the $\alpha$D305A mutant behaves similarly, then the findings of Tsai et al. (*47*) rule out a mechanism involving the release of $\alpha$-aminoacrylate via the nucleophilic attack of $\beta$Lys 87, followed by the nonenzymatic hydrolysis of $\alpha$-aminoacrylate to pyruvate.

In the $\beta$D305A mutant, the Ala side chain methyl group is unable to fulfill the requirements for salt bridge formation with either $\beta$Arg 141 or $\beta$Lys167, and its smaller size makes it very likely that the $\beta$-site in the mutant enzyme is always solvent accessible regardless of the protein conformation. The fact that, in the presence of BZI, pyruvate formation is almost completely inhibited implies that BZI binding stabilizes a $\beta$-site conformation that provides steric protection of the $\alpha$-aminoacrylate Schiff base. Owing to the structural

similarity of indole to BZI, it seems likely that the conformation of the (BZI)E(A−A) complex is essentially identical to the reactive (indole)E(A−A) complex, thus rendering the BZI complex an obvious target for structure determination.

Scheme 2C shows that free α-aminoacrylate is the likely reactant for inactivation of the βD305A mutant. The greater solvent accessibility of the β-site in the mutant enzyme may promote hydrolysis of the E-(A−A) intermediate and lead to mechanism-based inactivation. The PLP absorbance band at 412 nm slowly disappears when the reaction with L-Ser is performed in the presence of $Na^+$ or GP (Figure 1). When the pH of the solution is raised to 13, the 412 nm band is replaced by a broad peak at 424 nm (*41*) (Scheme 2C). This behavior was first observed in studies of the mechanism-based inactivation of aspartate aminotransferase and glutamate decarboxylase (*39*, *40*). This type of inactivation has also been demonstrated for several mutant forms of tryptophan synthase including βD305N, and βS377D (*41*, *42*).

*Implications of E(Aex$_1$) Stabilization and Impaired Quinonoid Formation in the βD305A Mutant.* Figure 2 (panels A and C) compare UV−vis static spectra for stage I of the β-reaction for the wild-type enzyme and for the βD305A mutant. These spectra establish that in contrast to wild-type enzyme (panel A), the mutant (panel C) favors the E(Aex$_1$) species (open conformation) over the E(A−A) species (closed conformation), both in the presence and in the absence of allosteric effectors. These spectra show that $Na^+$ has a remarkable stabilizing effect on the more open conformation of the E(Aex$_1$) species. The results obtained for the reaction of L-Ser and indoline, with the mutant (Figure 2, panels B and D) reflect the same behavior seen in stage I of the β-reaction. A significant amount of E(Q)$_{indoline}$ ($\lambda_{max}$ 466 nm) only accumulates in the presence of $Cs^+$. Furthermore, the quinonoid formed with the mutant enzyme is not very stable, and the absorbance at 466 nm completely disappeared after 30 m. The $Na^+$ form greatly stabilizes the E(Aex$_1$) species. As found for the $Na^+$ form, in the presence of $K^+$, $NH_4^+$, GP, or the combination of $NH_4^+$ and GP, only trace amounts of E(Q)$_{indoline}$ accumulate.

These experiments establish that the replacement of βAsp305 by Ala affects the ability of the enzyme to undergo the chemical and conformational transitions that accompany interconversion of the E(Aex$_1$) and E(A−A) species. Although a nearly wild-type-like steady-state kinetic behavior is restored in the $Cs^+$-form of the mutant, the step in which the α-proton is extracted is not completely repaired by $Cs^+$ or by any of the other allosteric effectors. The isotope effects resulting from replacement of [α-$^1$H]L-Ser by [α-$^2$H]L-Ser show that abstraction of the α-proton in the mutant enzyme dominates the rate-limiting step (Table 3). These apparent KIEs range between 3.1 and 6.2. The wild-type enzyme exhibits a rather high KIE only in the presence of $Na^+$ (5.0) or $K^+$ (3.0). The rates for the formation and decay of E(Aex$_1$) are very slow in comparison to the wild-type enzyme (Figure 3 and Table 2). The $Na^+$ and $K^+$ forms of βD305A show essentially no decay of the E(Aex$_1$) species. In the presence of $NH_4^+$ or $Cs^+$, or in the absence of MVCs, some decay is seen but these relaxations are ∼10-fold slower than in the wild-type system. The KIEs in Table 3 and the static spectra reported in Figure 2 indicate that the absence of a decay phase for the $Na^+$ and $K^+$ forms is the consequence of an unfavorable reaction equilibrium in stage I for formation of E(A−A).

*βD305A Mutation Alters β-Site Substrate Specificities.* Reaction with the L-Ser analogue DAPA and titrations with L-Ser were investigated to explore the substrate specificity of the mutant enzyme for the natural substrate. Figure 6A shows the reaction of wild-type enzyme with DAPA in the presence of $Cs^+$. The slow increase in absorbance at 350 nm concomitant with the decrease at 412 nm, are spectral changes characteristic of a slow formation of the E(A−A). In contrast with the wild-type enzyme, reaction of the $Cs^+$-form of βD305A with DAPA shows no spectral change (Figure 6B). When the concentration of DAPA is increased to 200 mM (Figure 6C), the mutant shows spectral changes very similar to those seen in the reaction of wild-type enzyme with 40 mM DAPA (Figure 6A).

Titration of wild-type enzyme with L-Ser shows a $K_{D,app}$ of 0.074 mM. The presence of BZI or $Cs^+$ lowers $K_{D,app}$, but the effects are rather small (3.2- and 1.6-fold respectively, and 6.7-fold when combined) (Table 4 and Figure 5). The L-Ser titrations for the βD305A mutant enzyme show much larger $K_{D,app}$ values than those seen in the wild-type system. Both in the presence of BZI and in the presence of BZI plus $Cs^+$, the $K_{D,app}$ values (0.80 and 0.18 mM, respectively) are almost 20 times greater than those for the wild-type system.

Both the experiments with DAPA and the titrations with L-Ser show that the apparent affinity of the mutant enzyme for substrate is significantly lower than that of the wild-type enzyme. The stopped-flow fluorescence experiments (Figure 3 and Table 2) show the rates for the formation and the decay of the E(Aex$_1$) species in stage I of the β-reaction, in the β-reaction and in the overall αβ-reaction, both for the mutant and for the wild-type systems. In the presence of $Na^+$ or $K^+$, or in the absence of MVCs, the rates for E(Aex$_1$) formation with βD305A are substantially lower than in the wild-type enzyme system, whereas the difference is smaller in the presence of $NH_4^+$ or $Cs^+$. Again, the rate of E(Aex$_1$) formation reflects a combination of the binding affinity for the substrate and the chemical steps, and, therefore, is not a direct probe of enzyme affinity for L-Ser; however, the results are in qualitative agreement with those mentioned above. Together, these results and the X-ray structure studies (PDB file 1BEU) suggest a catalytic role for Asp 305 in the recognition of substrate, presumably via H-bonding to the hydroxyl group of the L-Ser external aldimine. This interaction can be satisfied by the $NH_2$ group of Asn in the βD305N mutant (*13*), but not by the methyl group of Ala in the βD305A mutant.

In the reaction of L-Ser with indoline, the $Na^+$ form of βD305A does not accumulate E(Q)$_{indoline}$ in detectable amounts, but instead stabilizes the E(Aex$_1$) species (Figure 2D). Accumulation of E(Q)$_{indoline}$ is substantial for the $Cs^+$ form, whereas the MVC-free form and the $K^+$, $NH_4^+$, GP, and GP plus $Na^+$ forms give only trace amounts. The behavior of the wild-type enzyme is very different: the β-sites are converted to E(Q)$_{indoline}$ in high yield in the presence of $Na^+$, $Na^+$ plus GP, or $Cs^+$. However, GP or $NH_4^+$ are less effective, and the MVC-free enzyme gives only trace amounts. The spectral and kinetic data presented in Figure 2 and Table 2 indicate that the diminished ability of the mutant to form E(Q)$_{indoline}$ is primarily due to a destabilization of the closed conformation of the β-site rather

than to a shift in the relative rates for $E(Q)_{indoline}$ formation and decay.

Studies with the $\beta$D305N mutant (*13*, *41*, *49*) and this work establishes that the carboxylate of Asp 305 is not strictly necessary for the formation of $E(Q)_{indoline}$, but substitution with Ala strongly decreases its stability. The X-ray structure of the $\beta$K87T mutant enzyme in the form of $E(Aex_2)$ (Figure 7, panels B and C) shows that the plane of the indole ring of the L-Trp aldimine is oriented perpendicular to the ring of $\beta$Phe 306 and is in van der Waals contact with it. This interaction strongly indicates that the ring of $\beta$Phe 306 imposes strict steric constraints for the attack of indole on the E(A−A) species. Mutation of Asp 305 to Ala surely affects the position of the Phe 306 side chain, and this change in geometry consequently affects the stability of the quinonoid species. Therefore, the carboxylate of Asp 305 does not play a critically important chemical bonding role in the catalytic mechanism, but rather functions in modulating the conformational state of the $\beta$-active site.

*$\beta$D305A Mutation Alters Quinonoid Stability.* In the wild-type system, the quinonoids formed with indole, aniline, hydroxylamine, *N*-methylhydroxylamine, and phenylhydrazine are stable for at least half an hour, whereas in the $\beta$D305A mutant these quinonoidal species completely disappear under the same conditions (Figure 4). In the wild-type system, indoline is the only known nitrogen-based nucleophile that turns over (albeit slowly) in the presence of L-Ser to give detectable amounts of a new amino acid, while the quinonoidal species formed with other nitrogen-based nucleophiles do not (*1*, *44*). The behavior of the $\beta$D305A mutant shows that the formation and decay of these quinonoids is due to conversion to new amino acids. *Consequently, the failure of the corresponding wild-type enzyme quinonoids to undergo conversion to new amino acids has protein conformational origins.*

Reaction of $\beta$D305A with L-Ser and BZI shows that this analogue (as in the wild-type system) fails to react covalently but, instead, stabilizes the E(A−A) species through formation of a noncovalent complex (*44*). The inability of BZI to react with E(A−A) is postulated to have its origins in the stereoelectronic control of nucleophilic attack imposed by the site on the geometry of the E(A−A) complex with BZI (*1*, *2*, *44*).

The behavior of the $\beta$D305A mutant in the reactions between L-Ser and the nitrogen-based indole analogues provides a striking contrast with the wild-type system, where only indoline turns over to produce detectable amount of a new amino acid, DIT.

An hypothesis that explains the high selectivity of tryptophan synthase toward these nucleophiles may be found by considering the reaction mechanism with particular attention to the structure of the quinonoids formed with indole and the other nucleophiles. All of these nucleophiles form quinonoidal species with H-bonding capabilities not present in $E(Q_3)$ (eq 4)

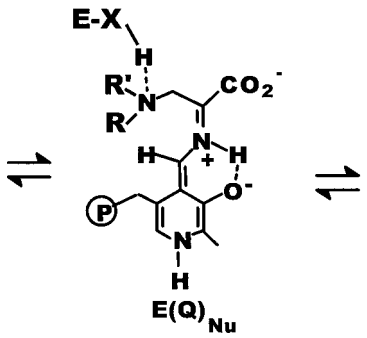


(4)

where R = aryl or alkyl and R′ = alkyl or H.

These studies indicate that formation of the $\beta$D305−$\beta$R141 salt bridge is important for stabilization of the closed conformation of the quinonoidal intermediates. Suppose in the wild-type system that within the closed conformation, a site residue forms a (catalytically inappropriate) H-bond of weak to moderate strength with these E(Q) species (3−8 kcal/mol) that is not present in the indole quinonoid system (eq 4). If this H-bond must be broken before conversion to the open structure of the corresponding external aldimine can occur, then this H-bond would create a substantial energy barrier for conversion to the next intermediate. Accordingly, both the H-bonding interaction and the closed protein conformation associated with the $\beta$D305−$\beta$R141 salt-bridge would contribute stability to these quinonoids. Since the $\beta$D305A mutant cannot form the salt bridge to $\beta$R141, substitution of Asp with Ala destabilizes the closed conformation of the mutant $E(Q_{Nu})$ species, allowing conversion to the new amino acids to occur.

*Structure−Function Relationships Revealed by the $\beta$D305A Mutation.* The structures presented in Figure 7, panels A−C, show the location of PLP, ligands, and residues $\beta$302−306 of two different X-ray structures of tryptophan synthase, the E(Ain) and the $\beta$K87T mutant of $E(Aex_2)$. The open conformation of the E(Ain) structure (Figure 7A) shows the two orientations for the side chain of Asp 305 proposed by the crystallographers (Hyde, C. C., et al.; PDB file 1BKS). In one conformation, $\beta$Asp 305 points toward $\beta$Arg 141 but is too distant (5.56 Å) to form a strong coulumbic interaction and is solvent exposed; in the other, the carboxylate points toward $\beta$Ala 302 and makes a salt bridge to $\beta$Lys 167 (not shown). In the structure of $E(Aex_1)$ (*16*), $\beta$Asp 305 is located within H-bonding distance of the hydroxyl group of the bound L-Ser substrate. The structure of $E(Aex_2)$ (Figure 7B) shows $\beta$Asp 305 is H-bonded to $\beta$Arg 141 in a salt bridge, an interaction which appears to stabilize a closed conformation that blocks access from solution into the $\beta$-site. From analysis of these structures, we conclude that $\beta$Asp 305 plays a role in the formation of $E(Aex_1)$ via H-bonding to the L-Ser hydroxyl as E(GD) is converted to $E(Aex_1)$. When the hydroxyl group of $E(Q)_1$ eliminates to form the E(A−A), the H-bonding interaction between the reacting substrate and $\beta$Asp 305 is lost, and $\beta$Asp 305 is free to rearrange in the E(A−A) complex to make an H-bonded salt bridge with $\beta$Arg 141 as the closed conformation is formed, thereby protecting the E(A−A) species by closing the $\beta$-site, and preventing access of water. According to mechanism A of Scheme 2, the exclusion of water prevents production of pyruvate from reaction of the E(A−A) species with water and provides a nonaqueous environment for the conversion to $E(Aex_2)$. The Asp to Ala mutation gives an enzyme that is unable to make the salt bridge with Arg 141, thereby leaving the $\beta$-site always solvent accessible, with the consequence of a high rate of pyruvate and ammonia formation. This hypothesis is in agreement with the "open-closed" mechanism proposed for the regulation of catalysis and channeling (*1*−*3*, *5*, *6*, *9*−*11*, *13*, *23*−*25*). A related "open-closed" mechanism was first proposed by Ahmed et

al. (*41*) to explain the elevated rate of pyruvate formation and the mechanism-based inactivation observed with several mutant forms of tryptophan synthase including βD305N.

In summary, these studies of the βD305A mutant enzyme provide new insights into the relationship between structure and function for the tryptophan synthase bienzyme complex and suggest new loci (e.g., βArg 141 in the β-subunit) for detailed mechanism studies. Moreover the broadened specificity due to the βD305A mutation introduces the use of tryptophan synthase mutants for the efficient production of unusual new L-amino acid analogues of L-Trp and/or L-Ser from the reaction of nucleophiles with the E(A−A) intermediate.

## REFERENCES


1. Dunn, M. F., Aguilar, V., Brzovic, P. S., Drewe, W. F., Jr., Houben, K. F., Leja, C. A., and Roy, M. (1990) *Biochemistry 29*, 8598−8607.
2. Brzovic, P. S., Sawa, Y., Hyde, C. C., Miles, E. W., and Dunn, M. F. (1992) *J. Biol. Chem. 267*, 13028−13038.
3. Brzovic, P. S., Ngo, K., and Dunn, M. F. (1992) *Biochemistry 31*, 3831−3839.
4. Leja, C. A., Woehl, E. U., and Dunn, M. F. (1995) *Biochemistry 34*, 6552−6561.
5. Pan, P., and Dunn, M. F. (1996) *Biochemistry 35*, 5002−5013.
6. Pan, P., Woehl, E., and Dunn, M. F. (1997) *Trends Biochem. Sci. 22*, 22−27.
7. Peracchi, A., Mozzarelli, A., and Rossi, G. L. (1994) *Biochemistry of Vitamin B6 and PQQ* (Marino, G., Sannia, G., and Bossa, F., Eds.) pp 125−129, Birkauser Verlag, Basel, Switzerland.
8. Peracchi, A., Mozzarelli, A., and Rossi, G. L. (1995) *Biochemistry 34*, 9459−9465.
9. Woehl, E. U., and Dunn, M. F. (1995) *Biochemistry 34*, 9466−9476.
10. Woehl, E. U., and Dunn, M. F. (1999) *Biochemistry 38*, 7118−7130.
11. Woehl, E. U., and Dunn, M. F. (1999) *Biochemistry 38*, 7131−7141.
12. Rhee, S., Parris, K. D., Ahmed, S. A., Miles, E. W., and Davies, D. R. (1996) *Biochemistry 35*, 4211−4221.
13. Weber-Ban, E., Banik, U., Hur, O., Bagwell, C., Miles, E. W., and Dunn, M. F. (2001) *Biochemistry 40*, 3497−3511.
14. Miles, E. W., Rhee, S., and Davies, D. R. (1999) *J. Biol. Chem. 274*, 12193−12196.
15. Brzovic, P. S., Hyde, C. C., Miles, E. W., and Dunn, M. F. (1993) *Biochemistry 32*, 10404−10413.
16. Rhee, S., Parris, K. D., Hyde, C. C., Ahmed, S. A.,, Miles, E. W., and Davies, D. R. (1997) *Biochemistry 36*, 7664−7680.
17. Yanofsky, C., Crawford, I. P. (1972) in *The Enzymes* (Boyer, P. D., Ed.) 3rd ed., pp 1−31, Academic Press New York.
18. Miles, E. W. (1979) *Adv. Enzymol. Relat. Areas Mol. Biol. 49*, 127−186.
19. Miles, E. W. (1995) Proteins: Structure, Function and Protein Engineering. In *Subcellular Biochemistry* (Biswas, B. B., and Roy, S., Eds.) Vol. 24, pp 207−254, Plenum Press, New York.
20. Hyde, C. C., Ahmed, S. A., Padlan, E. A., Miles, E. W., and Davies, D. R. (1988) *J. Biol. Chem. 263*, 17857−17871.
21. Dunn, M. F., Roy, M., Robustell, B., and Aguilar, V. (1987) in *Proceedings of the 1987 International Congress on Chemical and Biological Aspect of Vitamin B6 Catalysis* (Korpela, T., and Christen, P., Eds) pp 171−181, Birkhauser Verlag, Basel, Switzerland.
22. Kirschner, K., Weischet, W., and Wiskocil, R. L. (1975) in *Protein−Ligand Interactions* (Sund, H., and Blaver, G., Eds.) pp 27−44, Walter de Gruyter, Berlin.
23. Houben, K. F., and Dunn, M. F. (1990) *Biochemistry 29*, 2421−2429.
24. Dunn, M. F., Aguilar, V., Drewe, W. F., Jr., Houben, K., Robustell, B., and Roy, M. (1987) *Ind. J. Biochem. Biophys. 24*, 44−51.
25. Brzovic, P. S., Miles, E. W., and Dunn, M. F. (1991) in *Proceedings of the 8th International Congress on Vitamin B6 and Carbonyl Catalysis* (Wada, H., Soda, K., Fukui, T., and Kagamiyama, H., Eds.) pp 277−279, Pergamon Press, New York.
26. Peracchi, A., Bettati, S., Mozzarelli, A., Rossi, G. L., Miles, E. W., and Dunn, M. F. (1996) *Biochemistry 35*, 1872−1880.
27. Bahar, I., and Jernigan, R. L. (1999) *Biochemistry 38*, 3478−3490.
28. Kawasaki, H., Bauerle, R., Zon, G., Ahmed, S. A., and Miles, E. W. (1987) *J. Biol. Chem. 262*, 10678−10683.
29. Miles, E. W., Kawasaki, H., Ahmed, S. A., Morita, H., Morita, H., and Nagata, S. (1989) *J. Biol. Chem. 264*, 6288−6296.
30. Yang, L −H., Ahmed, S. A., and Miles, E. W. (1996) *Protein Expression Purif. 8*, 126−136.
31. Yang, L −H., Ahmed, S. A., Rhee, S., and Miles, E. W. (1997) *J. Biol. Chem. 272*, 7859−7866.
32. Weischett, W. O., and Kirschner, K. (1976) *Eur. J. Biochem. 65*, 365−373.
33. Dunn, M. F., Bernhard, S. A., Anderson, D, Copeland, A., Morris, R. G., and Roque, J. P. (1979) *Biochemistry 18*, 2346−2354.
34. Koerber, S. C., MacGibbon, A. K. H., Dietrich, H., Zeppezauer, M., and Dunn, M. F. (1983) *Biochemistry 22*, 3424−3431.
35. Drewe, W. F., Jr., and Dunn, M. F. (1985) *Biochemistry 24*, 3977−3987.
36. Drewe, W. F., Jr., and Dunn, M. F. (1986) *Biochemistry 25*, 2494−2501.
37. Brzovic, P. S., Holbrook, E. L., Greene, R. C., and Dunn, M. F. (1990) *Biochemistry 29*, 442−451.
38. Bernasconi, C. (1976) *Relaxation Kinetics*, Academic Press, New York.
39. Ueno, H., Likos, J. J., and Metzler, D. E. (1982) *Biochemistry 21*, 4387−4393.
40. Likos, J. J., Ueno, H., Feldhaus, R. W., and Metzler, D. E. (1982) *Biochemistry 21*, 4377−4386.
41. Ahmed, S. A., Ruvinov, S., B., Kayastha, A., M., and Miles, E. W. (1991) *J. Biol. Chem. 266*, 21540−21557.
42. Jhee, K. H., McPhie, P., Ro, H. S., and Miles, E., W. (1998) *Biochemistry 37*, 14591−14604.
43. Fan, Y., K., McPhie, P., and Miles, E. W. (2000) *J. Biol. Chem. 275*, 20302−20307.
44. Roy, M., Keblawi, S., and Dunn, M. F. (1988) *Biochemistry 27*, 6698−6704.
45. Schneider, T. R., Gerhardt, E., Lee, M., Liang, P.-H., Anderson, K. S., and Schlichting, I. (1998) *Biochemistry 37*, 5394−5406.
46. Sachpatzidis, A., Dealwis, C., Lubetsky, J. B., Liang, P. H., Anderson, K. S., and Lolis, E. (1999) *Biochemistry 38*, 12665−12674.
47. Tsai, M.-D., Schleicher, E. Potts, R., Skye, G. E., and Floss, H. (1978) *J. Biol. Chem. 253*, 5344−5349.
48. Miles, E. W. (1986) Pyridoxal Phosphate enzymes catalyzing β-elemination and β-replacement reaction. In *Pyridoxal Phosphate and Derivatives* (Dolphin, D., Poulson, R., and Avramovic, O., Eds.) pp 253−310, Wiley, New York.
49. Miles, E. W., Ahmed, S. A., and Kayastha, A. M. (1991) in *Enzymes dependent on pyridoxal phosphate and other carbonyl compounds as cofactors; proceeding of the 8th international symposium on vitamin B6 and carbonyl catalysis* (Fukui, T., Kagamiyama, H., Soda, K., and Wada, H., eds) pp 249−256, Pergamon Press.


BI002892L